A HIGH-Q BIRDBATH RESONATOR GYROSCOPE (BRG)

J. Cho, J.-K. Woo, J. Yan, R. L. Peterson, and K. Najafi
Center for Wireless Integrated MicroSensing and Systems (WIMS^2)
University of Michigan, Ann Arbor, Michigan, USA

ABSTRACT

We report a three-dimensional (3-D) micro-scale shell gyroscope made of fused silica (FS), called the birdbath resonator gyroscope (BRG). The BRG operates at 10.45 kHz, far above most environmental noise frequencies, and offers high mechanical quality factor ($Q_{n=2}$ = 249k) and low stiffness and damping anisotropy ($\Delta f_{n=2}$ = 14 Hz, $\Delta 1/\tau_{n=2}$ = 4.1 mHz). The birdbath (BB) resonator can be fabricated with good structural symmetry because its anchor is self-aligned to the rest of the structure. The BB resonator also has large frequency separation between the n=2 wineglass modes and the closest parasitic mode ($|f_{parasitic} - f_{n=2}|/f_{n=2}$ = 0.3), which makes the gyro less sensitive to vibration. The BRG is fabricated using a 3-D μ-blow-torching process and assembly on an electrode substrate made with the Silicon-On-Glass (SOG) process. The BRG is operated in the force-rebalance mode at <1 mTorr vacuum and room temperature, and has a scale factor of 27.9 mV/(deg/sec), a full-scale range >400 deg/sec, an angle random walk (ARW) of 0.106 deg/√hr and a bias stability of 1 deg/hr.

KEYWORDS

Gyroscope, birdbath, fused silica, quality factor (Q), blow-torch molding, silicon-on-glass (SOG), rate-integrating

INTRODUCTION

Many MEMS gyroscopes have been developed over the last two decades, and their resolution and accuracy have continuously improved. Recently, there has been increasing interest in the development of micro rate-integrating gyroscope (RIG). The RIG has advantages over the conventional rate gyroscope (RG) due to its direct angular readout, larger bandwidth, and larger dynamic range. The key challenge for RIGs, however, is that its bias drift is a direct function of the differences in the frequency (Δf) and inverse decay time ($\Delta 1/\tau$) of its two resonance modes. Therefore RIGs require an axisymmetric geometry with a very long τ. An alternative method for a rate gyro to achieve both large dynamic range and bandwidth based on the measurement of change in the oscillation frequency caused by the Coriolis force is suggested in [1-2]. However, this method similarly requires a gyro with a long τ and well-matched f for accurate phase detection, which makes it equally challenging to develop such a sensor.

Silicon RIGs made using conventional MEMS processes have been previously reported. A 2-kHz quad-mass tuning-fork gyroscope with a decay time constant τ >100 seconds and excellent resolution is reported in [3]. Its main drawback is its low operating frequency, which degrades its vibration sensitivity. Our group reported a multi-ring Si cylindrical gyro [4] with τ ~10 seconds, and a resonant frequency of 3 kHz. Its main drawback is the small angular gain (A_g = 0.013) due to its small height-to-radius ratio (H/R = 0.05). The wineglass mode frequencies ($f_{n=2}$) of above two example devices are designed to be <3 kHz to minimize thermoelastic damping (TED). For a Si beam gyroscope, τ_{TED} increases as the beam width decreases and f decreases [5]; however, the sensor becomes more sensitive to environmental vibration.

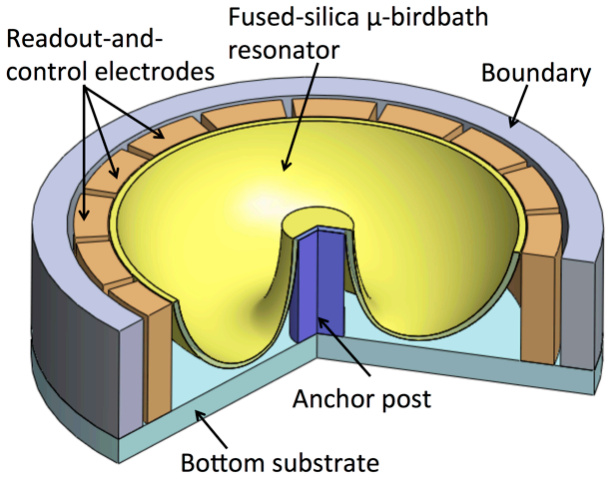

Figure 1: Structure of birdbath resonator gyroscope (BRG).

Fused silica (FS) has several attractive features over Si. Due to its smaller linear expansion coefficient (α_{FS} = 0.5×10^{-6} K^{-1} [6]) and thermal conductivity (k_{FS} = 1.38 $Wm^{-1}K^{-1}$ [6]), the τ_{TED} of a FS beam increases with beam thickness, regardless of f. FS is an amorphous material so it does not lose energy at grain boundaries [7] and has higher fracture toughness than Si ($K_{IC}(FS)$ = 0.88 MPa-$m^{1/2}$ [8]). Because of these advantages FS is used in the state-of-art macro-scale gyroscope, the Hemispherical Resonator Gyroscope (HRG), which has Q of several tens of millions [9]. However, the fabrication of a high-Q (>100k) micro FS resonator is challenging due to the difficulties in etching and depositing thick shells, and in achieving small surface roughness. It is also challenging to mold FS because its softening temperature ($T_{softening}$ = 1585 ºC [8]) is well above the temperatures of conventional MEMS processes. We recently overcame this challenge with a novel micro-scale blow-torch molding process [10]. The process utilizes a fuel-oxygen blow torch, which can provide intense amount of heat (up to 2500 °C) in a very short duration (<10 seconds) to reflow thin FS substrates (thickness ~ 100 μm) into a variety of 3-D geometries with a large device height (~2 mm).

In this paper, we demonstrate, for the first time, a micro-scale FS shell gyroscope, named the birdbath resonator gyroscope (BRG). The birdbath (BB) resonator is fabricated using the micro blow-torching process and is

assembled on to a separate electrode substrate made with the Silicon-on-Glass (SOG) process. We discuss the gyro architecture, fabrication process, and the evaluation results of the BRG.

DEVICE ARCHITECTURE

Figure 1 shows the structure of the BRG. It consists of a suspended FS birdbath resonator and 16 discrete electrodes surrounding its outer perimeter. The electrodes are designed for the control and measurement of the n=2 wineglass modes. The birdbath resonator is mounted face-up on an anchor post. In this way, it is easier to change the f and Q of the resonator. The electrodes and anchor are formed on a glass substrate.

The µ-birdbath (BB) resonator [11] offers several attractive features over the µ-hemispherical resonator [12]. First, the anchor and the rest of the shell are self-aligned, that is, they are formed using only a single patterning step, which leads to better structural symmetry and lower anchor loss. The µ-hemispherical resonator needs at least two patterning steps to define the shell geometry and the anchor, and the misalignment between the shell and anchor leads to larger anchor loss. Second, the BB resonator can also be mounted to the anchor either face up or down, which makes electrode integration and fabrication more compatible with different processes.

Table I: Frequency characteristics, angular gain (A_g) and effective mass (M) of BRG calculated with FEM.

µ-Birdbath 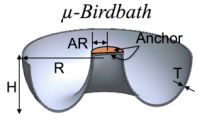	R = 2.5 mm AR = 0.5 mm H = 1.55 mm T_{rim} = 70 µm $\Delta T/\Delta H$ = 0.038 µm/µm
$f_{n=2}$	12.6 kHz
$f_{tilting}/f_{n=2}$	0.3
$f_{vertical}/f_{n=2}$	0.7
Effective mass (M)	680 µg
Angular gain (A_g)	0.25
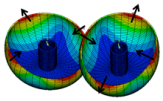 n=2 Wineglass mode	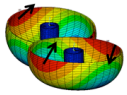 Tilting mode	 Vertical mode

Table I summarizes frequency characteristics, effective mass (M), and angular gain (A_g) of the BRG obtained using FEM [13]. The resonator has an outer radius (R) of 2.5 mm, an anchor radius (AR) of 0.5 mm, a rim thickness (T_{rim}) ~70 µm, and height (H) ~1.55 mm (H/R ~ 0.62). In the FEM model, the thickness of the shell (T) decreases linearly with vertical position, h, along the shell (where h=0 at the rim and h=H at the bottom of the resonator) with a ratio ($\Delta T/\Delta h$) of 0.038 µm/µm, i.e.

$$T(h) = T_{rim} - 0.038 \times h,$$

for a 100-µm thick FS substrate, to approximate the different amount of plastic deformation occurring in the FS substrate at different depths during molding.

We find that $f_{n=2}$ is determined mostly by R and T_{rim}; $f_{tilting}/f_{n=2}$ and $f_{vertical}/f_{n=2}$ are determined mostly by T at the bottom of the shell (T_{min}); and M is determined mostly by R and T_{rim}. The BB resonator has wide frequency separation between the n=2 wineglass modes and the closest parasitic mode ($|f_{parasitic} - f_{n=2}|/f_{n=2}$ = 0.3), and it can be further increased by using a thicker FS substrate. The large separation between these frequencies makes the BRG more immune to external vibration. Angular gain (A_g) is a parameter determined by the geometry and directly affects the scale factor of a gyro. From the FEM simulation, it is found that A_g is determined mostly by the height-to-radius ratio (= H/R). The A_g of the BRG reaches a maximum value of 0.3 when H/R ~ 1. With the current device geometry (H/R = 0.62), A_g is calculated to be 0.25.

FABRICATION PROCESS

A BB resonator is fabricated from a 100-µm FS substrate using a micro blow-torch-molding process and is metallized with sputtered Cr/Au (100/1000 Å) as described in [10]. Figure 2 describes the fabrication process of the electrode substrate and resonator assembly. Trenches of 1.6-mm depth are etched by deep reactive ion etching (DRIE) of a 2-mm low-resistivity (P-type) Si (Step 2a). A 4µm-thick Al protection layer is evaporated to cover the top surface, sidewall and bottom surface of the trenches. The Al layer is patterned using wet etching. The Si wafer is anodically bonded face-down to a 500-µm borosilicate wafer with 3-µm deep recesses in locations where the Si will be released in a later step. The wafers are bonded at 400 °C and a voltage of 1500 V (Step 2b). Si is removed with DRIE from the topside, leaving Si electrodes and anchor post (Step 2c). The Al protection layer is etched away in dilute hydrochloric acid, releasing the Si pieces located between the anchor post and the electrodes (Step 2d). The resonator is attached to the anchor post using polymer adhesive (Crystalbond™ 509, SPI Supplies, West Chester, PA, USA). The anchor tightly fits the resonator, which helps to self-align the resonator to the electrodes (Step 2e). Figure 3 shows a completed BRG. The sensor measures 8 mm (width) × 8 mm (length) × 2.5 mm (height). Figure 4 shows a close-up SEM of the 13.9 µm gap between the resonator shell and electrodes. The average electrode gap size (g_{avg}) across the 16 electrodes is 14.2 µm. The capacitance between the resonator and each electrode is measured

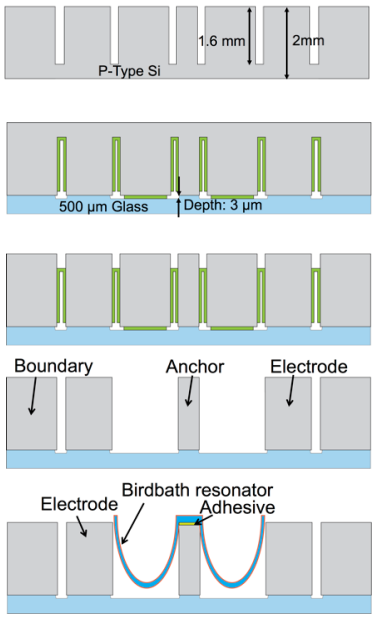

(a) Define 1.6 mm-deep DRIE trenches.

(b) Evaporate and pattern 4 µm thick Al protection layer. Anodically bond to borosilicate wafer with 3µm recess patterns.

(c) Etch the remaining thickness of Si.

(d) Dissolve protection layer.

(e) Metallize birdbath resonator. Assemble resonator to the electrode substrate.

Figure 2: Fabrication process steps for the micro birdbath resonator.

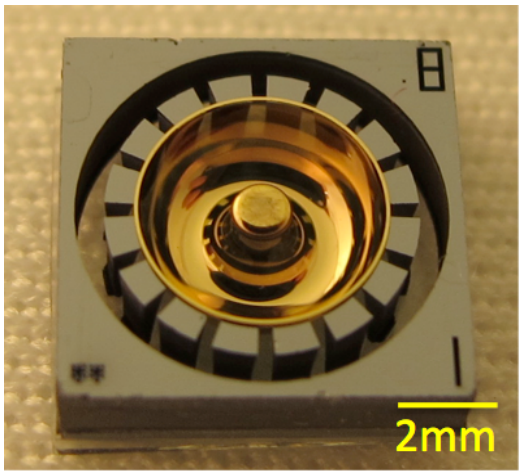

Figure 3: Birdbath Resonator Gyro (BRG) [Resonator size: radius (R) = 2.5 mm, anchor radius (AR) = 0.5 mm, height (H) = 1.55 mm. Device size: 8 mm (width) × 8 mm (length) × 2.5 mm (height)].

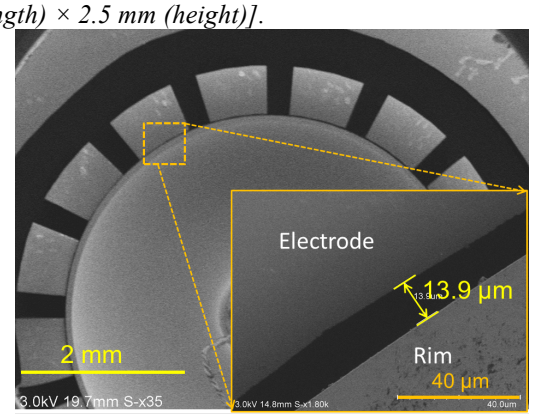

Figure 4: Close-up scanning electron microscope (SEM) image of the gap between shell and electrode (gap size = 13.9 µm).

with a HP 4284A Precision LCR Meter and is 153 ~ 182 fF. The capacitance variation may not cause any error in the force-rebalance mode, because the direction of the oscillation is nearly constant regardless of rotation rate; however, the capacitance variation is believed to cause bias instability in rate-integrating mode due to error in the control electrostatic force that disrupts the direction of the oscillation pattern.

DEVICE EVALUATION

Mode Characterization

The BRG is tested at <1 mTorr and room temperature. The n=2 wineglass modes are at 10,465 and 10,479 Hz ($\Delta f_{n=2}$ = 14 Hz, $\Delta f_{n=2}/f_{n=2}$ = 0.13%). The mode frequencies are electronically matched to less than 0.2 Hz, and further tuning is done using a quadrature cancellation loop. Figure 5 shows the decay time constant plot of one of the n=2 wineglass modes when their frequencies are separated by 0.22 Hz ($f_{n=2}$ = 10457.23 kHz and 10457.45 kHz). The $\tau_{n=2}$ are calculated by actuating the sensor at those frequencies, stopping the actuation, recording the decaying amplitudes, and fitting the recorded amplitudes with inverse exponential functions, i.e. $A_o exp(-t/\tau)$. The $\tau_{n=2}$ are measured to be 7.45 seconds ($Q_{n=2}$ = 244.75k) and 7.69 seconds ($Q_{n=2}$ = 252.64k). The anisotropy of the inverse of $\tau_{n=2}$ ($\Delta 1/\tau_{n=2}$) is 4.1 mHz.

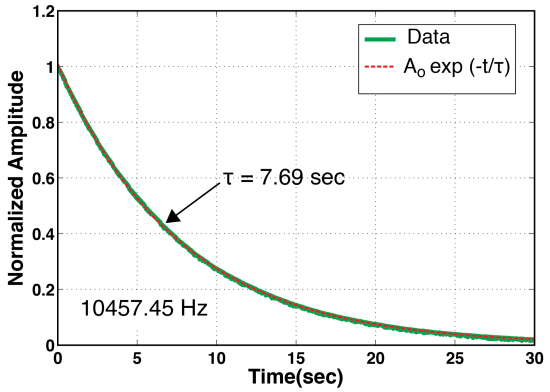

Figure 5: Decay time constant plots of one of the n=2 wineglass mode when their frequencies are closely tuned ($\Delta f_{n=2}$ = 0.22 Hz): $f_{n=2}$ = 10.45745 kHz, $\tau_{n=2}$ = 7.69 seconds ($Q_{n=2}$ = 252,640). [The other mode: $f_{n=2}$ = 10.45723 kHz, $\tau_{n=2}$ = 7.45 seconds ($Q_{n=2}$ = 244,750)]

Force-Rebalance Mode Control

The BRG is operated in the force-rebalance mode (Figure 6). Three control loops are implemented: an amplitude control loop to keep the oscillation amplitude of the gyro constant along the drive axis, a quadrature cancellation loop to zero the amplitude of the motion along the sense axis that is in a quadrature phase with the motion along the drive axis, and a Coriolis feedback loop to zero the amplitude of the motion along the sense axis that is in phase with the motion along the drive axis. Phase lock loops (PLL) are used to create the in-phase and quadrature signals of the motion along the drive axis. The control algorithm is implemented using Zurich Instrument's HF2LI lock-in amplifier. DC voltages are used to bias the resonator body and electronically tune in-axis and cross-axis stiffness. The sensor is evaluated on an Ideal Aerospace® Aero900 rotation table.

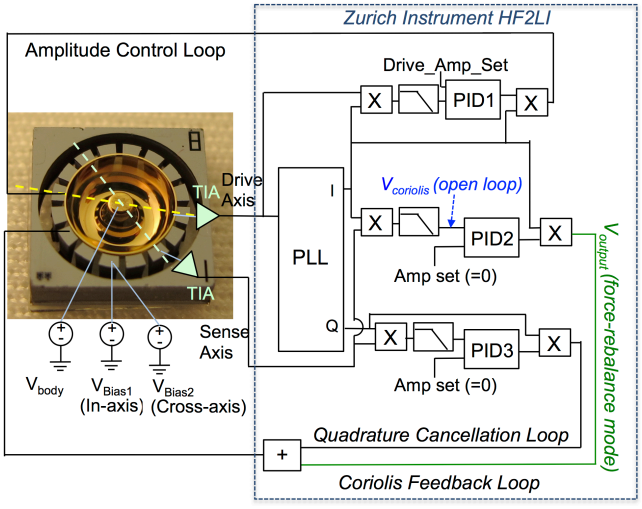

Figure 6: Interface/control algorithm diagram for the force-rebalance mode operation of the BRG.

Figure 7 shows the sensor response to DC rotation rate (Ω) from -125 to 125 deg/s. The scale factor is 27.8 mV/(deg/sec). The full-scale range of the sensor is found to be over 400 deg/sec. Figure 8 shows the Allan deviation plot, demonstrating an angle random walk (ARW) of 0.106 deg/√hr and a bias stability of 1 deg/hr. The low ARW and bias stability is attributed to the large

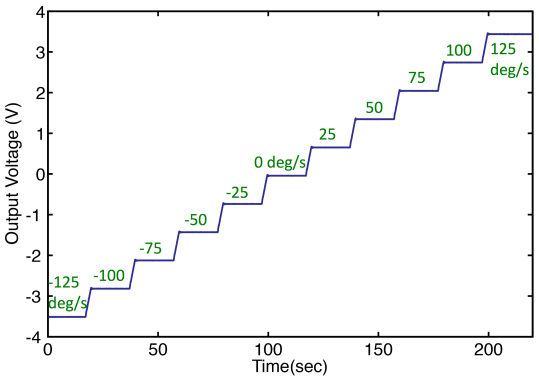

Figure 7: Sensor response to DC yaw rotation rate (Ω_z) of -125 to 125 deg/sec. The scale factor is 27.8 mV/(deg/sec). A full-scale range of over 400 deg/sec is measured.

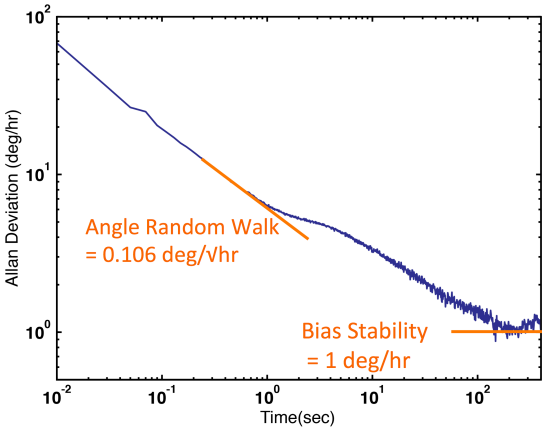

Figure 8: Allan Deviation plot of the BRG in force-rebalance mode: Angle random walk (ARW): 0.106 deg/√hr. Bias stability: 1 deg/hr.

Q of the BB resonator. In the future, the accuracy and stability can be further improved by reducing capacitive feedthrough, differential-mode sensing and actuation, more precisely controlling the operating temperature, and reducing the electrical noise in the bias sources.

Table 2: Design and testing summary

Parameters	
Resonator Dimension	*Radius (R): 2.5 mm, Height (H): 1.55 mm, Rim thickness (T_{rim}): ~70 μm*
Device size	*Device size: 8 mm (width) × 8 mm (length) × 2.5 mm (height)*
Frequency ($f_{n=2}$)	*10.465 kHz, 10.479 kHz*
Decay time constant ($\tau_{n=2}$)	*7.45 sec, 7.69 sec*
Angle random walk (ARW)	*0.106 deg/√hr*
Bias stability	*1 deg/hr*

SUMMARY

This paper reports the design, fabrication, and testing of a novel micro 3-D fused silica gyroscope, named the birdbath resonator gyroscope (BRG). The BRG operates at 10.45 kHz with high Q (= 249k) and has small stiffness and damping anisotropy ($\Delta f_{n=2}$ = 14 Hz, $\Delta 1/\tau_{n=2}$ = 4.1 mHz). The angular gain of the resonator is calculated by FEM to be 0.25. The prototype BRG is made by fabricating a BB resonator using a micro-blow torching process and assembling it on an electrode substrate made with the Silicon-on-Glass (SOG) process. The sensor is operated in the force-rebalance mode, and an angle random walk of 0.106 deg/√hr and a bias stability of 1 deg/hr are measured. Efforts are underway to develop the next-generation BRG with larger A_g, smaller stiffness and damping anisotropy, and small and uniform electrode gap. Table 2 summarizes the design and testing results of the BRG.

ACKNOWLEDGEMENTS

This work is supported by DARPA MRIG award #W31P4Q-11-1-0002. The authors thank Mr. Robert Gordenker for testing support. Portions of this work were done in Lurie Nanofabrication Facility (LNF), a site of the National Nanotechnology Infrastructure Network (NNIN), supported in part by the National Science Foundation (NSF).

REFERENCES

[1] S. A. Zotov *et al.*, "Frequency modulation based angular rate sensor," in *Proc. IEEE MEMS 2011*, pp. 577-580.

[2] M. H. Kline *et al*, "Quadrature FM gyroscope" in *Proc. IEEE MEMS 2013*, pp. 604-608.

[3] I. P. Prikhodko *et al.*, "Foucault Pendulum on a Chip: Angle Measuring Silicon MEMS Gyroscope," in *Proc. IEEE MEMS 2011*, pp. 161-164.

[4] J. Cho *et al.*, "High-Q, 3kHz Single-Crystal-Silicon Cylindrical Rate-Integrating Gyro (CING)," in *Proc. IEEE MEMS 2012,* pp. 172-175.

[5] R. Lifshitz and M. L. Roukes, "Thermoelastic damping in micro and nanmomechanical systems," *Phys. Rev. B*, vol. 61, n. 8, 2000, pp. 5600-5609.

[6] *HPFS Fused Silica Standard Grade Datasheet* [Online]. Available: http://www.corning.com/docs/specialtymaterials/pisheets/H0607_hpfs_Standard_ProductSheet.pdf.

[7] V. B. Braginsky, Systems with Small Dissipation. Chicago, IL: Univ. Chicago Press, 1985.

[8] C.B. Carter *et al. Ceramic materials: science and engineering*. New York, NY: Springer, 2007.

[9] E. J. Loper, Jr. and D. D. Lynch, "Vibratory Rotation Sensor," U.S. Patent 4,901,508, 1990.

[10] J. Cho *et al.*, "High-Q fused silica birdbath and hemispherical 3-D resonators made by blow torch molding," in *Proc. IEEE MEMS 2013,* pp. 177-180.

[11] K. Najafi and J. Cho, "Gyroscope and method of fabricating a resonator for a gyros," US Patent Application 13/481 650, May 25, 2012.

[12] L. D. Sorenson *et al.*, "3-D Micromachined Hemispherical Shell Resonators With Integrated Capacitive Transducers," in *Proc. IEEE MEMS 2012*, pp. 168-171.

[13] J. Cho, "High performance micromachined vibratory rate-and rate-integrating gyroscopes," Ph.D. thesis, Dept. EECS, Univ. Michigan, Ann Arbor, MI, 2012.

CONTACT

*K. Najafi, tel: +1-734-763-6650; najafi@umich.edu